2006

The cosmological significance of high-velocity cloud complex H

JD Simon

L Blitz

AA Cole

MD Weinberg

M Cohen

Accepted for publication in *The Astrophysical Journal*
Preprint typeset using LaTeX style emulateapj v. 6/22/04

THE COSMOLOGICAL SIGNIFICANCE OF HIGH-VELOCITY CLOUD COMPLEX H

Joshua D. Simon[1,2], Leo Blitz[1], Andrew A. Cole[3], Martin D. Weinberg[4], and Martin Cohen[5]

Accepted for publication in The Astrophysical Journal

ABSTRACT

We have used new and archival infrared and radio observations to search for a dwarf galaxy associated with the high-velocity cloud (HVC) known as Complex H. Complex H is a large ($\Omega \gtrsim 400$ deg^2) and probably nearby ($d = 27$ kpc) HVC whose location in the Galactic plane has hampered previous investigations of its stellar content. The H I mass of the cloud is $2.0 \times 10^7 (d/27 \text{ kpc})^2$ M$_\odot$, making Complex H one of the most massive HVCs if its distance is more than ~ 20 kpc. Virtually all similar H I clouds in other galaxy groups are associated with low surface brightness dwarf galaxies. We selected mid-infrared sources observed by the MSX satellite in the direction of Complex H that appeared likely to be star-forming regions and observed them at the wavelength of the CO $J = 1 \rightarrow 0$ rotational transition in order to determine their velocities. 59 of the 60 observed sources show emission at Milky Way velocities, and we detected no emission at velocities consistent with that of Complex H. We use these observations to set an upper limit on the ongoing star formation rate in the HVC of $\lesssim 5 \times 10^{-4}$ M$_\odot$ yr^{-1}. We also searched the 2MASS database for evidence of any dwarf-galaxy-like stellar population in the direction of the HVC and found no trace of a distant red giant population, with an upper limit on the stellar mass of $\sim 10^6$ M$_\odot$. Given the lack of evidence for either current star formation or an evolved population, we conclude that Complex H cannot be a dwarf galaxy with properties similar to those of known dwarfs. Complex H is therefore one of the most massive known H I clouds that does not contain any stars. If Complex H is self-gravitating, then this object is one of the few known dark galaxy candidates. These findings may offer observational support for the idea that the Cold Dark Matter substructure problem is related to the difficulty of forming stars in low-mass dark matter halos; alternatively, Complex H could be an example of a cold accretion flow onto the Milky Way.

Subject headings: Galaxy: evolution — galaxies: dwarf — Local Group — infrared: ISM — infrared: stars — radio lines: ISM

1. INTRODUCTION

What determines whether a low-mass gas cloud or dark matter halo becomes a dwarf galaxy or fails to undergo any star formation, remaining dark for billions of years? The answer to this question may underlie the substructure problem in Cold Dark Matter (CDM) cosmologies — the dramatic mismatch between the number of dark matter minihalos produced in numerical simulations and the number of dwarf galaxies observed in the Local Group (Klypin et al. 1999; Moore et al. 1999). Many possible explanations for why low-mass halos might not form stars have been proposed (e.g., Efstathiou 1992; Scannapieco, Ferrara, & Broadhurst 2000; Bullock, Kravtsov, & Weinberg 2000; Scannapieco, Thacker, & Davis 2001; Somerville 2002; Verde, Oh, & Jimenez 2002; Dekel & Woo 2003; Kravtsov, Gnedin, & Klypin 2004), but the existence of very low-mass dwarfs today suggests that this problem is not yet fully understood. One approach to improving our understanding of the formation of dwarf galaxies is to study extreme objects in order to determine what makes them unique. In this paper we investigate the nature of Complex H, an unusually massive high-velocity cloud (HVC) located in the Galactic plane (see Figure 1).

Complex H is centered on HVC 131+1−200, which was first discovered by Hulsbosch (1971) and Dieter (1971). Wakker & van Woerden (1991) noted that this HVC seems to be associated in position and velocity with a large number of other clouds, and named the grouping Complex H after Hulsbosch. The complex subtends 478 deg^2 (Wakker & van Woerden 1991) and extends in velocity all the way from $V_{\rm LSR} = -230$ km s^{-1} down to $V_{\rm LSR} \approx -120$ km s^{-1} where it begins to blend into Milky Way emission. The H I column density at the center of the cloud is $\gtrsim 2\times 10^{20}$ cm^{-2}, and the column is at least 2.0×10^{19} cm^{-2} for most of the central 25 deg^2. Complex H has an integrated H I mass of $\approx 2.7 \times 10^4 \, d_{\rm kpc}^2$ M$_\odot$, where $d_{\rm kpc}$ is the distance to Complex H in kiloparsecs (Wakker et al. 1998, hereafter W98). Ivezic & Christodoulou (1997) used IRAS data to search for star formation in Complex H and found one candidate young stellar object, but this source is likely to be a foreground Milky Way object.

W98 examined ultraviolet spectra of 17 OB stars for interstellar absorption lines of Mg II, C II, and O I in the direction of Complex H. They detected no absorption near the velocity of Complex H and concluded that even

[1] Department of Astronomy, 601 Campbell Hall, University of California, Berkeley, CA 94720-3411; jsimon@astro.berkeley.edu, blitz@astro.berkeley.edu
[2] Current address: Department of Astronomy, MS 105-24, California Institute of Technology, Pasadena, CA 91125; jsimon@astro.caltech.edu
[3] Kapteyn Astronomical Institute, University of Groningen, Postbus 800, 9700 AV Groningen, the Netherlands; cole@astro.umn.edu
[4] Department of Physics and Astronomy, University of Massachusetts, Amherst, MA 01003; weinberg@astro.umass.edu
[5] Radio Astronomy Laboratory, 601 Campbell Hall, University of California, Berkeley, CA 94720-3411; mcohen@astro.berkeley.edu

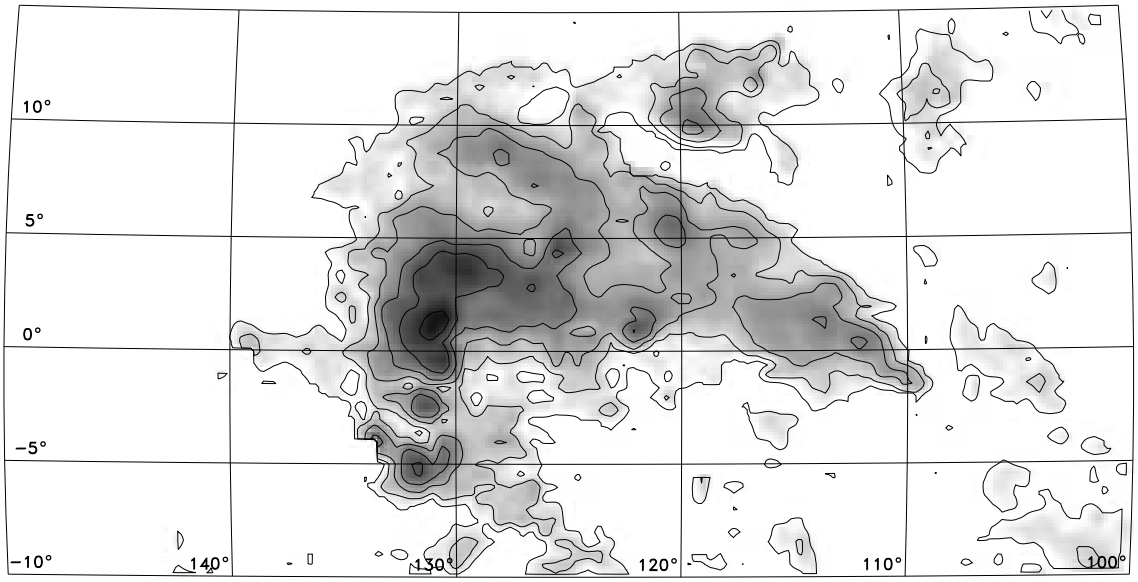

FIG. 1.— H I map of Complex H in Galactic coordinates from the Leiden/Dwingeloo Survey of Galactic Neutral Hydrogen (Hartmann & Burton 1997). The image shows the integrated intensity for velocities between -230 km s^{-1} and -150 km s^{-1}. The contours are spaced logarithmically and correspond to column densities of 4.6×10^{18} cm^{-2}, 9.2×10^{18} cm^{-2}, 1.8×10^{19} cm^{-2}, 3.7×10^{19} cm^{-2}, 7.3×10^{19} cm^{-2}, and 1.5×10^{20} cm^{-2}. The Dwingeloo telescope has a beam size of $36'$ and the survey was carried out with a grid spacing of $30'$.

for substantially subsolar abundances, the HVC must be located beyond the farthest of the stars they studied. They placed a firm lower limit of 3.4 kpc on the distance to Complex H. Since the distances of some of the OB stars are rather uncertain, the actual minimum distance could be as large as 6.5 kpc. Blitz et al. (1999) additionally pointed out that the velocity of Complex H is too large for it to be in circular rotation around the Galaxy at any distance. They further argued that the lack of any observational evidence for an interaction between Complex H and the interstellar medium of the Milky Way strongly implies that the HVC must be located beyond the edge of the disk of the Galaxy, at least $\sim$ 20 kpc away from the Sun. Since Complex H has velocities of up to 100 km s^{-1} with respect to the nearest Galactic gas, strong shocks and X-ray and radio emission would be produced if it were located within the H I disk of the Milky Way. The most recent H I observations of Complex H by Lockman (2003) do indicate that the HVC is beginning to interact with the Milky Way, but this interaction takes the form of tidal stripping of Complex H's outer layers rather than the high-energy collision that would be occurring if Complex H were closer than the edge of the disk.

Lockman (2003) further noticed that the velocity gradient across the cloud in the b (Galactic latitude) direction can be used to derive its vertical motion relative to the Galaxy. Using H I maps from the Green Bank Telescope, he constructed a model of Complex H and argued that the HVC is in an inclined, retrograde orbit around the Milky Way. These calculations place Complex H 33 ± 9 kpc from the Galactic center and 27 ± 9 kpc from the Sun. More general distance constraints can be derived by considering the aforementioned lack of a strong interaction between Complex H and the Milky Way, and the total mass of the cloud. The Milky Way disk gas extends out to a minimum Galactocentric distance of 27 kpc at the position of Complex H (Blitz et al. 1999), placing a firm lower limit of 21 kpc on the distance between the HVC and the Sun if the cloud lies just beyond the edge of the disk. At distances of more than 100 kpc, Complex H would be the fourth most massive object in the Local Group, which seems unlikely since no counterpart at other wavelengths has been detected. The full range of plausible distances is therefore $21 - 100$ kpc, corresponding to H I masses of $1.2\times 10^7 - 2.7 \times 10^8$ M$_\odot$.

Because starless extragalactic gas clouds as large as Complex H are not seen in other groups of galaxies (with only one exception [Minchin et al. 2005]), it seems reasonable to suppose that Complex H is the H I component of a previously undiscovered dwarf galaxy. At the distance of 27 kpc preferred by Lockman (2003), Complex H would have an H I mass, total mass (assuming that it is gravitationally bound), and physical extent that are consistent with those of other Local Group galaxies.

Before we proceed, the issue of the total mass of Complex H deserves some comment. If the HVC is actually a dwarf galaxy, a baryon fraction of 0.04 (typical for dwarf galaxies) would imply a total mass of $\sim 5 \times 10^8$ M$_\odot$. In a ΛCDM cosmology, such a dark matter halo should have a peak circular velocity of at least ~ 30 km s^{-1}. Neither the velocity gradient across the cloud (which in the Lockman model is attributable to the orbital velocity of the HVC rather than its internal motions) nor the velocity dispersion of the gas is nearly this large, so the kinematics of the cloud do not require a total mass this high. Nevertheless, if the H I extent of the cloud is smaller than the scale radius of the dark matter halo, the ob-

served kinematics would not be expected to reflect the full gravitational potential of the halo.

We now consider the possibilities for confirming or refuting the presence of a dwarf galaxy in Complex H. The V-band extinction in the direction of the center of the HVC is estimated to be 4 magnitudes (Schlegel, Finkbeiner, & Davis 1998), although the calculated extinction near the Galactic plane is subject to significant uncertainties. The combination of heavy extinction and severe crowding makes an optical detection of a distant group of stars very difficult (although not impossible, as was illustrated by the detection of the Sagittarius dwarf spheroidal behind the Galactic center by Ibata, Gilmore, & Irwin 1995). Instead, we shall search for evidence of a dwarf galaxy at longer wavelengths where both the extinction and the crowding are less severe or nonexistent. Specifically, we use mid-infrared observations from the Midcourse Space Experiment (MSX) satellite to identify star-forming regions that could be associated with Complex H. We then employ millimeter-wave CO observations to determine the nature and location of these objects. These data should reveal the presence of massive stars in Complex H if any star formation has taken place in the last $\sim 10^7$ years. Other Local Group dwarf irregulars that have comparable H I masses to Complex H, such as Sextans B and IC 1613, are actively forming stars. In addition, we use the Two Micron All Sky Survey (2MASS) near-infrared database to search for stars in the putative dwarf galaxy, taking advantage of the order of magnitude decrease in extinction between V-band and K-band.

In the following section, we discuss the MSX dataset, present our new CO observations, and describe the results of our search for star formation. In §3 we describe our analysis of the 2MASS data and in §4 we consider the interpretation of our findings. Our conclusions are summarized in §5.

2. SEARCH FOR RECENT STAR FORMATION IN COMPLEX H

2.1. *MSX Data*

The MSX satellite (Mill et al. 1994) was a US Department of Defense mission, undertaken by the Ballistic Missile Defense Organization. Launched in 1996, the infrared instrument on board consisted of a 35-cm off-axis telescope with detectors in six mid-infrared bands (two very narrow near 4 μm, and four broad at roughly 8, 12, 15, and 21 μm). All sensors had pixels of 18.3″. The primary infrared product was a survey of the entire Galactic plane within $-5^\circ < b < 5^\circ$ and about 20″ (FWHM) resolution (Price et al. 2001). The MSX Point Source Catalog version 2.3 (PSC2.3) contains six-color infrared photometry for over 4.3×10^5 sources in the Galactic plane (Egan et al. 2003). The MSX data products that we use for our analysis have a 3 σ sensitivity limit for low surface brightness diffuse emission that varies across the field from $2 - 9 \times 10^{-7}$ W m^{-2} sr^{-1} and are sensitive to point sources with flux densities down to ≈ 100 mJy.[6]

2.2. *Detectability of Complex H in the Mid-IR*

If Complex H is indeed the gaseous counterpart of a dwarf galaxy, the galaxy could in principle be either a dwarf irregular (dIrr) or a dwarf spheroidal (dSph), although its gas content would be rather large for a dSph (Blitz & Robishaw 2000). The photospheres of individual stars in such a galaxy are much too faint to have been detected with MSX, since even an O star would have a flux density of less than 1 mJy at 8 μm for a distance of 27 kpc. However, H II regions containing warm dust can become much brighter; if dust in the vicinity of an O star is heated to a temperature of more than ~ 100 K, it will be easily visible with MSX. Emission from the polycyclic aromatic hydrocarbon (PAH) bands at 6.2 μm, 7.7 μm, and 8.7 μm in photodissociation regions could further enhance the detectability of such star forming regions, although the likely abundance of PAHs in this environment is quite poorly known.

Since all known dwarf irregular galaxies contain H II regions (with the exception of some of the transitional dwarfs), it is a reasonable expectation that Complex H might contain H II regions as well. In order to estimate the brightness of these star-forming regions, we used other Local Group dwarfs as a comparison. NGC 6822, IC 10, and the SMC have all been observed in the mid-infrared by MSX, the *Spitzer Space Telescope*, or both. These galaxies have approximately an order of magnitude more neutral gas than Complex H, but none of the lower-mass dwarfs has been observed yet at useful sensitivities and resolutions. Their metallicities are low, $Z = 0.1 - 0.3 Z_\odot$ (Chandar, Bianchi, & Ford 2000; Lequeux et al. 1979; Peimbert & Torres-Peimbert 1976), similar to what is seen in HVCs, so these galaxies are plausible proxies for Complex H. We examined five H II regions in these galaxies: Hubble V and Hubble X in NGC 6822, HL45 and HL106b (Hodge & Lee 1990) in IC 10, and N81 in the SMC. When scaled to a distance of 27 kpc, Hubble V and Hubble X are extremely bright, with 8 μm flux densities[7] of 32 Jy and 10 Jy, respectively. These two regions do have relatively high star formation rates ($\sim 10^{-3}$ M$_\odot$ yr^{-1}, estimated using the Kennicutt, Tamblyn, & Congdon [1994] relation between Hα luminosity and star formation rate), making them less than ideal comparison objects. The IC 10 H II regions and N81 may be more appropriate templates, with scaled 8 μm flux densities of 1.82 Jy, 3.25 Jy, and 0.81 Jy, respectively. The corresponding star formation rates are 7×10^{-5} M$_\odot$ yr^{-1} and 1×10^{-5} M$_\odot$ yr^{-1} in IC 10 (again calculated from the Kennicutt et al. relation) and 5×10^{-4} M$_\odot$ yr^{-1} in N81 (derived from *Hubble Space Telescope* observations of the OB stars in the region [Heydari-Malayeri et al. 1999] with extrapolation to low-mass stars from a Salpeter [1955] or Kroupa [2001] initial mass function). A final point of comparison comes from MSX observations of some of the most distant known molecular clouds in the outer Galaxy. Of the 11 clouds listed by Digel, de Geus, & Thaddeus (1994) at distances from the Sun between 10 and 21 kpc, 5 are detected by MSX, with 8 μm flux densities ranging from 108 mJy to 470 mJy. This demonstrates that faint H II regions at

[6] We only use the 8 μm data in this paper because of the much lower sensitivity in the longer wavelength bands.

[7] The 8 μm bands of *Spitzer* and MSX have somewhat different shapes and bandwidths, but their fluxes tend to agree within 20%, so we do not attempt any correction to put all of these observations on an identical scale.

similar distances to what we assume for Complex H are detectable in MSX data.

2.3. *Target Selection*

The 20″ resolution of the highest-resolution MSX data corresponds to a physical size of $0.097 d_{\rm kpc}$ pc, where $d_{\rm kpc}$ is the distance to Complex H in kiloparsecs. A typical H II region of diameter 50 pc would subtend an angle of 6.′4 at the nominal distance of 27 kpc to Complex H, and would thus be resolved easily by MSX. Ultracompact H II regions (less than 2 pc in diameter), however, would show up as point sources at distances of greater than ~ 20 kpc. Therefore, we consider both point sources and extended sources in our search for evidence of star formation in the HVC.

As a first step, we searched the PSC2.3 for evidence of an enhanced density of infrared point sources near the center of Complex H. The distribution of these sources in the plane of the Galaxy is displayed in Figure 2. Although there are a few overdensities close to the expected location, further investigation reveals that the string of sources from $\ell \approx 132^\circ - 138^\circ$ is associated with the Milky Way star forming complex W3/W4/W5 (e.g., Carpenter, Heyer, & Snell 2000) and the cluster at $\ell = 126.7^\circ$, $b = -0.8^\circ$ is the H II region Sharpless 187 (Sharpless 1959; Joncas, Durand, & Roger 1992). It is also worth noting that the average density on the sky of 8 μm point sources around $\ell = 131^\circ$, $b = 1^\circ$ (the core of the HVC) is very close to the mean value for the outer Galactic plane of about 20 deg^{-2}.

We then examined the area in question in more detail. The region of highest H I column density in the HVC is roughly bounded by $127^\circ < \ell < 133^\circ$ and $-1^\circ < b < 5^\circ$, so for simplicity we will assume that any star formation that has taken place in Complex H occurred in this area. The MSX band A (8 μm) deep mosaic image of this region is shown in Figure 3, along with H I data from the Leiden/Dwingeloo Survey (Hartmann & Burton 1997). This MSX image was extracted from a $10^\circ \times 10^\circ$ product with 36″ pixels and 72″ resolution, and has sensitivity limits given in §2.1.

We selected 43 of the brightest extended sources for follow-up observations based on a mosaic constructed of high-resolution (6″ pixels, 20″ resolution) MSX images covering the region displayed in Figure 3. It is clear from a casual inspection of the figure that the brightest infrared sources in this part of the sky are concentrated well away from the H I peak of Complex H. We therefore added 10 bright point sources located near the core of the HVC to our target list. Finally, we included seven IRAS sources (many of which were expected to be Galactic star-forming regions) from the compilation of Fich & Terebey (1996) in order to make sure that they were actually Milky Way objects and to confirm that our observing strategy could detect star-forming regions.

2.4. *CO Observations*

We observed our targets with the NRAO/UASO 12 m reflector on the days of 2000 May 5 – 9. At the wavelength of the CO $J = 1 \rightarrow 0$ line, the telescope has a beam width of 55″. We used the millimeter autocorrelator with a 300 MHz bandwidth and 0.2541 km s^{-1} resolution and two polarizations. System temperatures were between 300 and 500 K for most of our observations, and reached as high as 1000 K for a few scans as the HVC approached the horizon. Typical integration times were $8 - 12$ minutes per position, for a total observing time of $40 - 60$ minutes on each source. We observed in relative position–switching mode with beam throws of a few arcminutes and used the online vane calibration to set the antenna temperature scale. The telescope pointing and focus were checked approximately every six hours, or after sunrise and sunset. The data were reduced in COMB by subtracting a linear baseline from each spectrum and then combining the two polarizations. For the extended sources, we observed a five point cross pattern around each source, with the spacing of the points chosen to be slightly less than the radius of the source. For the point sources, we only observed a single position since the beam size of the 12 m telescope is larger than the resolution of the MSX data.

2.5. *Millimeter Search Results*

We observed the 60 targets shown in Figure 3 and examined the spectra for emission or absorption (emission in the off position) features in the velocity range -300 km s^{-1} $< V_{LSR} <$ 100 km s^{-1}. Milky Way objects should appear with velocities $V_{LSR} > -120$ km s^{-1}, and we expect Complex H emission to lie between -230 km s^{-1} and -170 km s^{-1} if any is present (velocities as high as -120 km s^{-1} are also possible, but less likely). We detected Milky Way CO lines in either emission or absorption toward all 43 of the MSX extended sources, nine out of the ten MSX point sources, and all seven of the Fich & Terebey H II regions, indicating that at least 59 of our 60 targets are almost certainly Milky Way star-forming regions. The only object that we did not detect, MSX6C G131.1875+00.4726, may be a Milky Way infrared source of some kind that does not contain any CO, or it could be that the molecular gas is simply offset enough from the infrared position that it lies outside the beam of the 12 m. We did not find any emission lines at velocities below -102 km s^{-1},[8] so there is no evidence that any of these targets are associated with Complex H.

In Table 1 we list the results of our CO observations for each source. Columns (1) and (2) contain the Galactic coordinates of the targets, column (3) contains the velocity centroids of the detected lines, column (4) contains the peak observed brightness temperatures (again, note that negative observed temperatures indicate the the emission was located in the off position), column (5) contains the integrated intensity of the line, and column (6) describes how the targets were selected. For many lines of sight multiple emission components were detected, so we include all lines with an integrated intensity that is significant at the 5 σ level or higher in this table. Note, however, that we frequently omit lines at local velocities (-10 km s^{-1} $\lesssim V_{LSR} \lesssim$ 5 km s^{-1}) when other components with more negative velocities are also detected along the same line of sight. Our compilation is therefore incomplete at these velocities, but this local material is not relevant for our purposes. The distribution of velocities that we find for the Milky Way

[8] Several spectra showed apparently significant features at lower velocities, but repeat observations failed to confirm the reality of these lines.

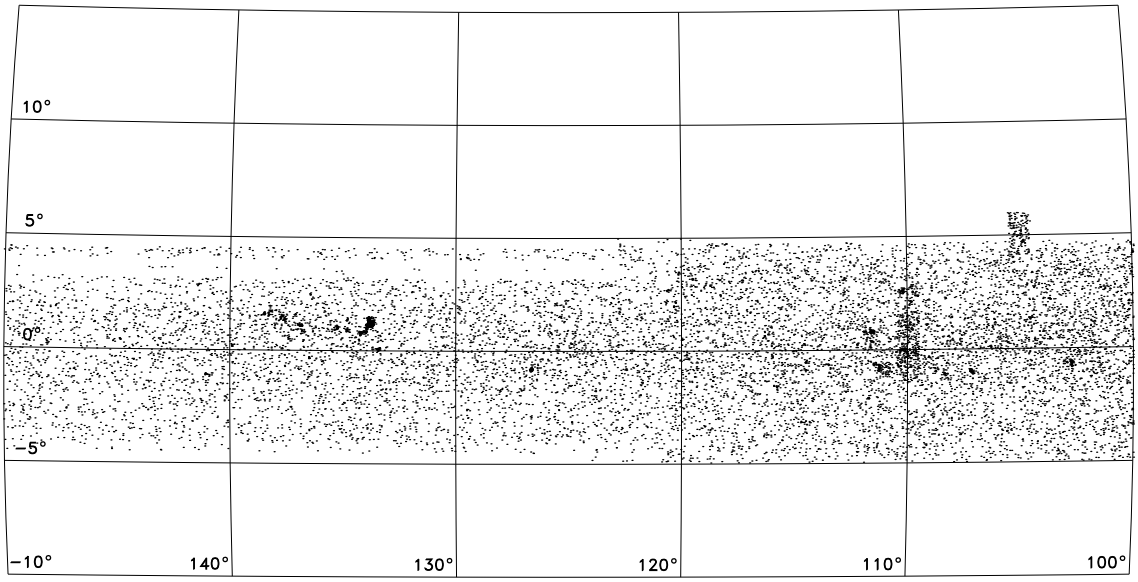

FIG. 2.— MSX point sources in the outer Galaxy. All sources listed in the Point Source Catalog (Egan et al. 2003) are plotted. Overdensities near the position of Complex H ($\ell = 131°, b = 1°$; see Figure 1) are visible, but they can all be identified with nearby Milky Way H II regions.

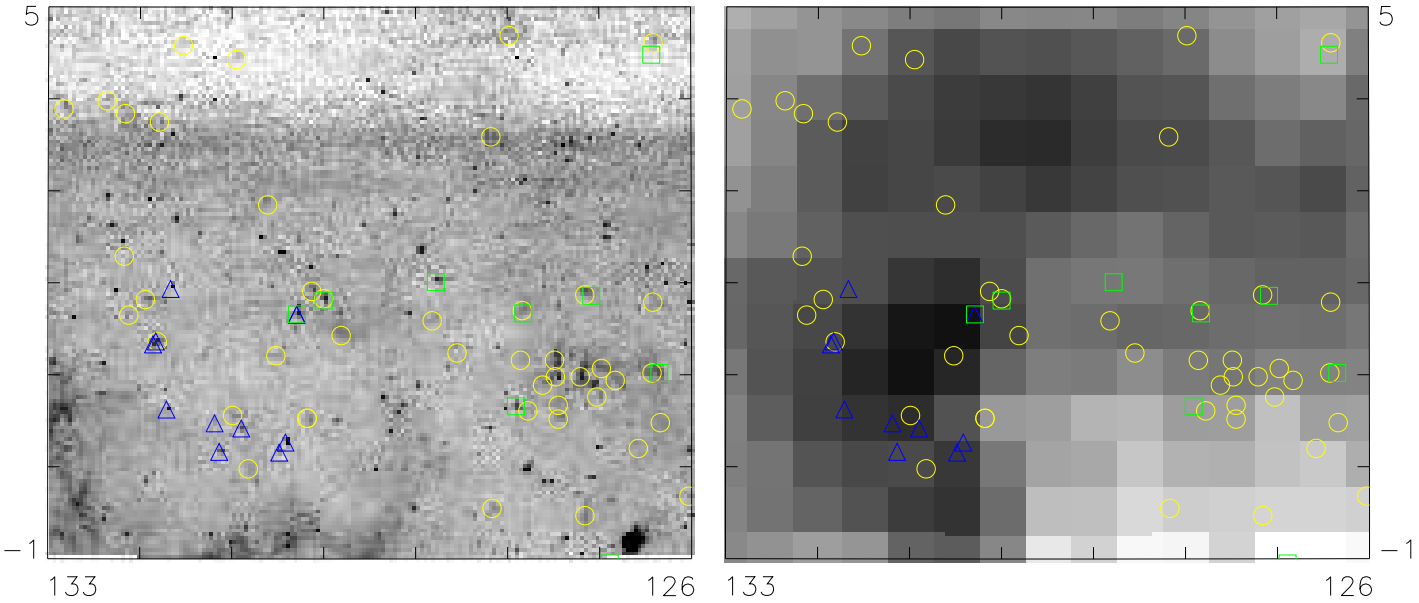

FIG. 3.— (a) MSX 8-μm deep mosaic image of the center of Complex H. The displayed region spans Galactic longitudes from 126° (right edge of the image) to 133° (left edge) and Galactic latitudes from −1° (bottom) to 5° (top). The sources we selected for followup observations are marked. Yellow circles represent MSX extended sources, blue triangles represent MSX point sources, and green squares represent IRAS sources from Fich & Terebey (1996). (b) H I image of the center of Complex H from the Leiden/Dwingeloo Survey. The angular coverage is the same as in panel (a). The infrared targets are overplotted as in panel (a). It is clear that the location of the H I peak of the HVC lies near a minimum of the infrared emission, suggesting that the MSX sources are not associated with Complex H.

clouds we detect is plotted in Figure 4. Distinct peaks in the distribution appear at velocities of −10 km s^{-1} (local material), −55 km s^{-1} (Perseus spiral arm), and −80 km s^{-1} (outer spiral arm).

Over the velocity range in which Complex H emission is most likely (-230 km s^{-1} $< V_{LSR} <$ -170 km s^{-1}), our spectra reach a typical rms of 0.05 K for extended sources and 0.13 K for point sources (because of the shorter integration times). Assuming a distance of 27 kpc and a linewidth of 6 channels (1.52 km s^{-1}), simi-

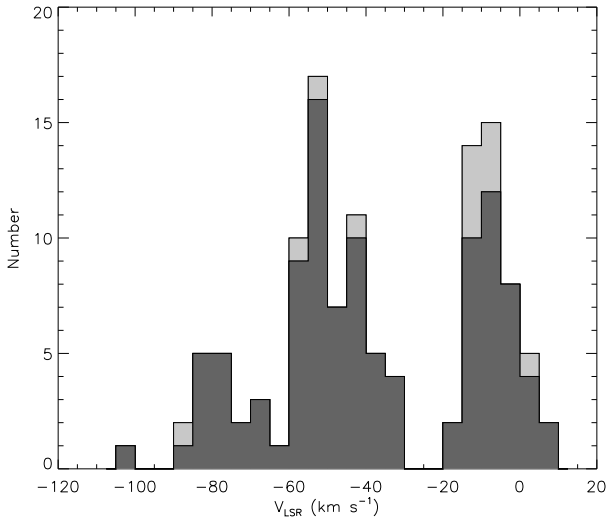

FIG. 4.— Velocity histogram of the Milky Way CO lines we detected. Emission lines are shown in dark gray and absorption lines (which actually represent emission in the reference position) are shown in light gray.

lar to the linewidths of the Galactic lines we detected, we translate these rms values to 3 σ upper limits on the total molecular mass associated with each source of $24-130$ M$_\odot$, with a median upper limit of 47 M$_\odot$. These masses correspond to typical molecular cores in Galactic star forming regions, but are much smaller than the masses of giant molecular clouds. These mass limits also assume that the Milky Way value of X_{CO}, the CO-H$_2$ conversion factor, is appropriate for Complex H. Recent analyses of X_{CO} in other galaxies suggest that it has at most a weak dependence on metallicity (Walter et al. 2001, 2002; Bolatto et al. 2003; Rosolowsky et al. 2003), which would validate our assumption.

In addition to searching for localized CO emission in Complex H, we can also combine all of our spectra to search for a very faint, diffuse component. Our spectra of 60 sources span 7° of longitude and 6° of latitude, covering a total area of approximately 0.05 deg^2 ($\sim 10^4$ pc^2 at a distance of 27 kpc) with a net integration time of 125 ks. The average spectrum over all of our observed positions has an rms noise level of 5 mK, which (again assuming the Galactic value of X_{CO} and a linewidth of 1.52 km s^{-1}) yields a 3 σ upper limit of ~ 1000 M$_\odot$ on the diffuse molecular content of the HVC.

2.6. *Limits on the Star Formation Rate in Complex H*

If we interpret these results as implying that there are currently no OB associations comparable to or larger than N81 in Complex H, then the observed OB star population of N81 suggests that the most massive star forming region in the HVC must have a star formation rate of less than 5×10^{-4} M$_\odot$ yr^{-1}. This limit holds as long as the distance to Complex H is less than ~ 75 kpc (the largest distance at which N81 would be visible in MSX images). Since it is unlikely that Complex H contains multiple H II regions just below this limit, this number also represents a plausible upper limit for the star formation rate of the entire cloud.

An alternate method to estimate the star formation that could be ongoing in Complex H without being detected in our data is to utilize the observed correlations between infrared and radio continuum flux densities and star formation rates in other galaxies. Cohen & Green (2001) showed that H II regions in the Milky Way have a mean ratio of 8 μm MSX emission to 843 MHz radio continuum emission of $R = 27 \pm 3$. Cohen et al. (2003) suggested that R values of ≈ 15 might be more appropriate for the LMC (and therefore for other dwarfs as well), but to place the most generous limits we will use the Milky Way value. It is well-known that the radio continuum luminosities of galaxies provide a good indicator of their star formation rates. Murgia et al. (2002) found that the star formation rate surface density (for stars more massive than 5 M$_\odot$) is $8.0 \times 10^{-4}\ B_{1.4}$ M$_\odot$ yr^{-1} kpc^{-2}, where $B_{1.4}$ is the observed flux density at 1.4 GHz in mJy/bm. Since the MSX flux limit is 100 mJy, our nondetection of any infrared sources associated with Complex H implies an upper limit to the 843 MHz radio flux density of any Complex H H II regions of 3.7 mJy. Filipovic et al. (1998) found approximately flat spectral indices for the radio continuum emission from LMC and SMC H II regions, so we assume that the 1.4 GHz flux density of H II regions in Complex H (if there are any) is also less than 3.7 mJy. The Murgia et al. star formation rate prescription then indicates that the star formation surface density in Complex H star-forming regions must be $\lesssim 3.0 \times 10^{-3}$ M$_\odot$ yr^{-1} kpc^{-2}. The 20″ MSX beam subtends an area of $5.4 \times 10^{-6}\ (d/27\ \mathrm{kpc})^2$ kpc^2, so the total star formation rate in any single Complex H H II region (after accounting for the contribution of low-mass stars down to 0.1 M$_\odot$ with a Salpeter initial mass function) has an upper limit of $\sim 1 \times 10^{-7}\ (d/27\ \mathrm{kpc})^2$ M$_\odot$ yr^{-1}. This calculation is much more restrictive than the one given in the previous paragraph, but without further knowledge of the infrared and radio properties of star-forming regions in very low-mass dwarf galaxies, it is difficult to assess which one provides a more meaningful limit.

By comparison, known Local Group dIrrs have star formation rates ranging from 1×10^{-4} M$_\odot$ yr^{-1} for the Sagittarius dwarf irregular galaxy, with an absolute magnitude of $M_V = -12.3$, up to nearly 1 M$_\odot$ yr^{-1} for IC 10, with an absolute magnitude of $M_V = -15.7$ (Mateo 1998, and references therein). The most similar dwarfs to Complex H in terms of H I mass have star formation rates of a few times 10^{-4} M$_\odot$ yr^{-1}. We conclude that the present-day star formation rate in Complex H is certainly no higher than that of other dwarf irregulars with similar masses, and there is some basis for arguing that it is substantially lower.

3. SEARCH FOR A DISTANT STELLAR POPULATION BEHIND THE MILKY WAY

Dwarf galaxies, whether they contain significant amounts of gas or not, usually have a substantial fraction of their stellar mass locked up in an old, metal-poor stellar population. Therefore, even though Complex H lacks appreciable amounts of massive star formation, we must also search for an evolved stellar population associated with the HVC. The most luminous stars in such a population are on the red giant branch (RGB) and the asymptotic giant branch (AGB). These stars can be easily recognized by their characteristic distribution in opti-

cal and near-infrared color-magnitude diagrams (CMDs). In the case of Complex H, optical data are largely useless because of the very high foreground density of Milky Way stars combined with several magnitudes of extinction. Near-infrared observations, in contrast, offer several strong advantages: much less extinction, lower foreground levels (since most stellar spectra peak at shorter wavelengths), and the enhanced brightness of RGB and AGB stars relative to other types of stars. In this section, we describe our use of 2MASS data to search for evidence of an ancient stellar population in Complex H.

3.1. *2MASS Data*

The 2MASS project surveyed the entire sky in three near–infrared bands (J, H, and K_S). 2MASS images have typical seeing of about $3''$, and the data are complete down to 10 σ limiting magnitudes of $J = 15.8$, $H = 15.1$, and $K_S = 14.3$ (2MASS Explanatory Supplement.[9]) In the near–infrared, the red giant branch extends up to $K_S \approx -6.2$ at a color of $J - K_S \approx 1$ (Nikolaev & Weinberg 2000), so a population of evolved stars is visible in the 2MASS dataset out to a distance modulus of $m - M \approx 20$ ($d = 100$ kpc). The 2MASS Point Source Catalog (Cutri et al. 2003) includes photometry and astrometry for $\sim 4.7 \times 10^8$ objects.

3.2. *Search Technique*

Using the 2MASS Point Source Catalog, we can construct color–magnitude diagrams (CMDs) of the center of Complex H. We search for a population of evolved stars behind the Milky Way by comparing these CMDs to those of nearby regions (e.g., at the same Galactic latitude but $\sim 10^\circ$ away in longitude). If the population is relatively massive (comparable to the Sagittarius dSph, for example), the RGB will be visually obvious in the CMD without even attempting to enhance the signal by statistically removing foreground stars. Low-mass dwarfs, on the other hand, can be difficult to detect.

In Figure 5 we display the K_S, $J - K_S$ CMD for a 1 deg^2 region centered on the peak of the HI distribution of Complex H ($\ell = 131^\circ, b = 1^\circ$). The two strong plumes of stars extending upward around $J - K_S = 0.4$ and $J - K_S = 1.0$ correspond to foreground main sequence stars and a mixture of Milky Way red clump and red giant branch stars, respectively. As shown in Figure 5*b*, a red giant population associated with Complex H would appear as a sequence of stars following the purple tracks up and to the right from the right side of the foreground giant branch (e.g., Cole 2001). Age differences only have a very small effect on the color of the dwarf galaxy giant branches, while a decrease in reddening or metallicity would move the tracks to the blue, increasing the possibility of confusion with the plume of foreground K giants. No feature that is immediately identifiable with a dwarf galaxy population is apparent, although there is a small scattering of stars fainter and redder than $(J - K_S, K_S) = (1.2, 13)$ that could conceivably be representatives of such a population. However, these stars could equally well be differentially reddened foreground K giants at distances of a few kiloparsecs.

To test the significance of this scattered population of faint red stars, we compared the Complex H field to a nearby control field. Because the sightline through the Galactic plane is subject to strong differential reddening, a random choice of control field can yield misleading results. We used MSX band A images to guide us to an appropriate control field, operating under the assumption that areas with low levels of emission from warm dust (which is visible at 8 μm) would also have low levels of differential reddening. On this basis, we selected a 1 deg^2 control field located at $\ell = 141^\circ, b = 2.2^\circ$. We show grayscale Hess diagrams of the Complex H and control fields in Figure 6 (left and center panels, respectively). As measured by the width of the foreground red giant branch and the number of highly reddened outliers, the two fields are indeed subject to similar amounts of differential reddening. We control for any difference in the mean reddening by measuring the color of the main-sequence stars in each field at $13 < K_S < 14$. The measured colors of $J - K_S = 0.52$ (Complex H) and $J - K_S = 0.67$ (control field) imply a difference in E(B-V) of 0.27 mag. We dereddened the control field by this amount and subtracted the two Hess diagrams, producing the difference image shown in the right panel of Figure 6. No coherent structure corresponding to a dwarf galaxy RGB is evident.

3.3. *Detection Limits*

In order to quantify the limits that the 2MASS data place on the stellar content of the HVC, we considered the detectability of various stellar populations in the 2MASS observations of Complex H. We first determined the surface brightness limit of the 2MASS point source catalog for the detection of resolved systems at various distances *along this particular sightline*. To do so, we calculated the number of excess stars necessary to constitute a 3 σ detection of a dwarf galaxy in the Complex H field that is not present in the control field. The star counts are related to V-band surface brightnesses using empirical K_S-band luminosity functions and starcount-surface brightness relations for dwarf spheroidals taken from the literature. Owing to the survey's rather shallow depth, we restrict our attention to the part of the CMD that we would expect to find populated with the red giant stars of a nearby dwarf galaxy. This isolates the relevant stars and suppresses noise from blue stars that are certain to be foreground objects. In raw terms, the detection limits on a stellar population are set by Poisson statistics: a galaxy of given surface brightness is expected to contain a certain number of RGB and AGB stars detectable by 2MASS. By comparing the control field + model dwarf galaxy starcounts to the Complex H starcounts, we can put a lower (bright) limit on the surface brightness of any possibly present dwarf.

Broadly speaking, there are two generic categories of dwarf galaxies: those with substantial intermediate-age populations (e.g., Fornax, Leo I, and the Sagittarius dSph), and those without (e.g., Sculptor, Ursa Minor, and Draco). Therefore we used two different sets of luminosity functions, color cuts, and starcount-surface brightness relations in our analysis. We modeled both types of dwarfs with a luminosity function (LF) of the same form, $N(K) \propto 10^{K/4}$ (Davidge 2000a,b). The luminosity functions are taken to be identical for magnitudes below the RGB tip ($K_S \approx -6.2$); brighter than this limit, the LF is assumed to drop by a factor of 3 in the

[9] http://www.ipac.caltech.edu/2mass/releases/allsky/doc/explsup.html

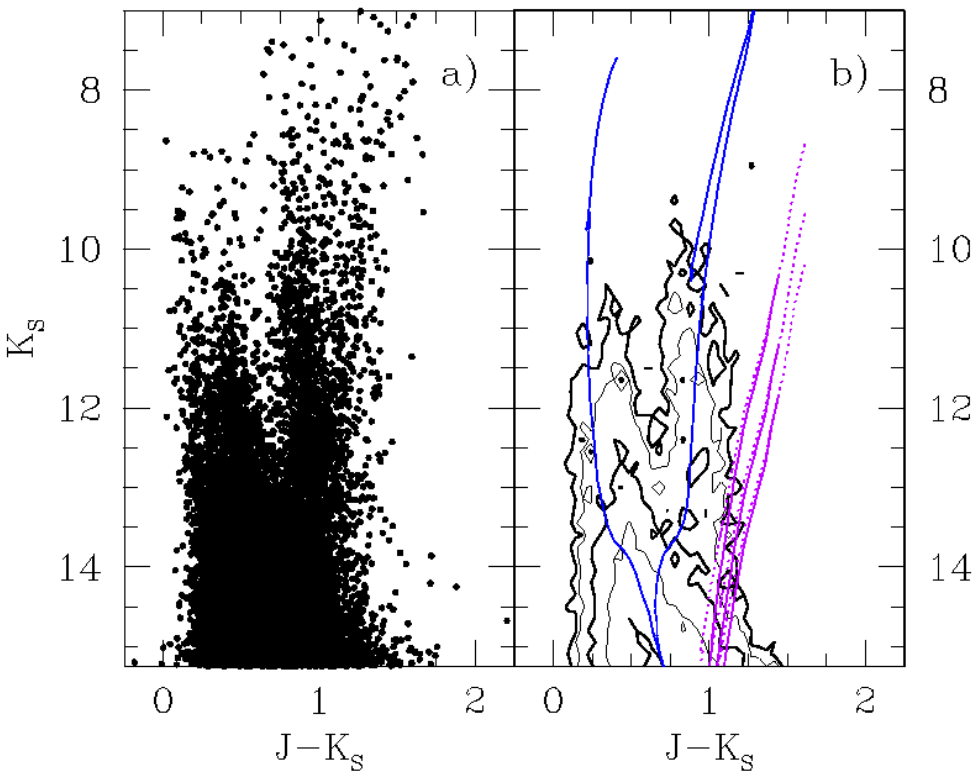

FIG. 5.— (a) 2MASS color-magnitude diagram of the center of Complex H. (b) 2MASS CMD (contours) with theoretical stellar isochrones overlaid. The stellar density is contoured with logarithmically spaced isopleths between 4 and 144 stars per 0.1 mag^2. The isochrones are based on the Padua set of stellar models (Girardi et al. 2000) and show the expected locations of Galactic and putative dwarf galaxy stellar populations in the diagram. Solar metallicity tracks ($Z = 0.019$) are shown in blue, and low-metallicity tracks ($Z = 0.004$) are displayed in purple. For display purposes, the high-metallicity tracks are shown for the single distance of 2 kpc (the approximate distance to the nearest spiral arm in this sightline; Gómez et al. 2002). The ages for these tracks are 100 Myr, to show the approximate location of the zero-age main sequence (the plume of stars with $J - K_S \lesssim 0.75$), and 10 Gyr, to give an approximate trace of the red giant branch populations (the redder plume with $J - K_S \approx 1.0$). A reddening equivalent to E(B-V) = 0.6 has been applied to the isochrones representing these relatively nearby populations. The primary features visible in the CMD are clearly caused by Milky Way main sequence and red giant stars present over a wide range of distances. The purple tracks show a relatively metal-rich ($[Fe/H] \approx -0.7$) dwarf galaxy population, with solid lines representing stars up to the tip of the red giant branch, and dotted lines to show the horizontal branch and AGB evolution. Three distances have been chosen for display, corresponding to the likely distance of Complex H: 18, 27, and 36 kpc. All three tracks have been plotted with the equivalent of 0.8 mag of foreground reddening, and an age of 4 Gyr.

mixed-age population, giving it a significant population of AGB stars. This model contains roughly equal fractions of old and intermediate-age stars, similar to Fornax (Saviane, Held, & Bertelli 2000). By contrast, the purely old population suffers a factor of 10 discontinuity at the tip of the RGB and therefore contains virtually no bright AGB stars.

The normalization factors and conversion to starcounts were taken from Irwin & Hatzidimitriou (1995), with our purely old galaxy typified by the Sculptor dSph, and using the Fornax dSph as our template for an intermediate-age dwarf. In making the conversion between galaxy surface brightness and predicted 2MASS starcounts it is important to consider the effect of incompleteness on the faint end of the luminosity function. We modeled incompleteness by multiplying the synthetic luminosity functions by a function proportional to $\tanh(K)$ to generate our starcount predictions.

We then computed lower limits to the surface brightness of a putative dwarf galaxy associated with Complex H for the adopted reddening (see §3.2) and for distances ranging from $10 - 160$ kpc. The results are shown in Figure 7, where the open circles represent our 3 σ detection limits for a dwarf galaxy dominated by an old stellar population at this position, and the open squares represent the same limit for a galaxy that also contains an intermediate-age component. Note that the shape of the detectability curves is very similar to those calculated by Willman et al. (2002a) for the *Sloan Digital Sky Survey* (SDSS), but the SDSS data probe ~ 2 mag deeper.

These calculations place a firm lower limit on the surface brightness of the old stellar content of Com-

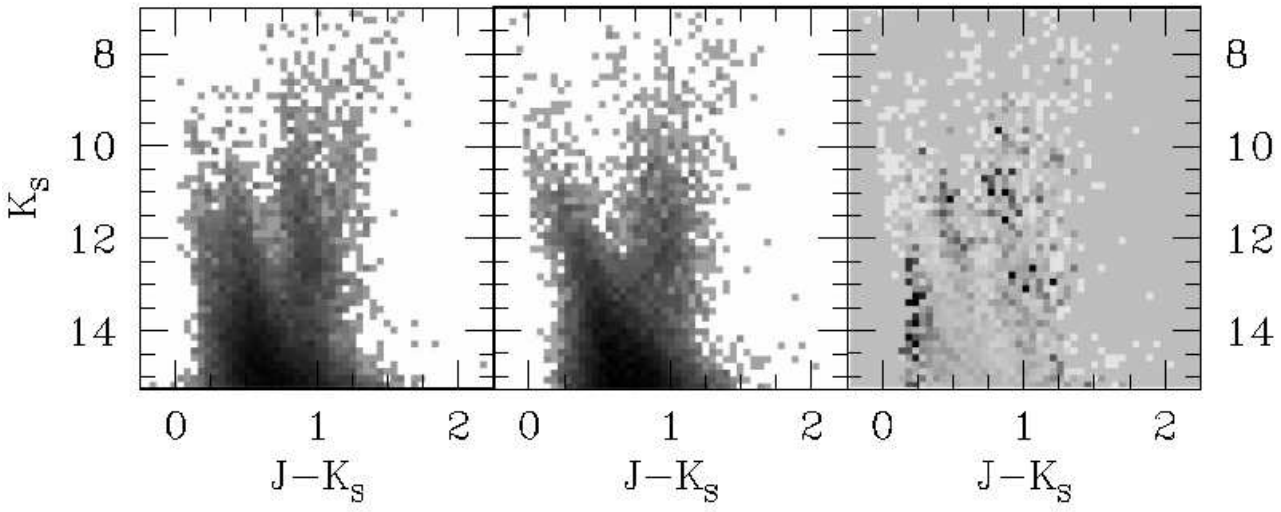

FIG. 6.— Hess diagrams of the 2MASS data in the direction of Complex H (left panel) and the control field (middle panel). The grayscale ranges from 0 counts per cell (white) to 125 counts per cell (black). The difference between the two Hess diagrams, after adjusting the reddening of the control field to match that of Complex H, is displayed in the right panel. The cells in the residual plot represent counts in the Complex H Hess diagram minus counts in the control field Hess diagram, as a fraction of the counts in the control field Hess diagram. The mean difference level is about 7%, and the grayscale ranges from −1% (white) to 10% (black). Although the residuals shows that the populations of the two fields are not identical, there is no coherent structure at the location where a red giant population at $d \sim 27$ kpc would be found (see Figure 5).

plex H of $\mu_V \geq 25.25$ mag arcsec^{-2}. Spread over our 1 deg^2 search area, the corresponding stellar luminosity is 6×10^5 L$_\odot$, implying an absolute upper limit to the stellar mass of Complex H of 1.2×10^6 M$_\odot$ for a typical V-band stellar mass-to-light ratio of 2. For a population covering a smaller area, the stellar mass limit is correspondingly lower. If Complex H contains an intermediate-age population, then the surface brightness limit is $\mu_V \geq 26.25$ mag arcsec^{-2}, at least 1 mag arcsec^{-2} fainter than that of the Sgr dSph and 2.5 mag arcsec^{-2} fainter than Fornax. No known dwarf irregular galaxies have such low surface brightnesses, and only $\sim 1/4$ of the currently known Local Group dwarf spheroidals are so faint. In the case of a purely old population of stars, a galaxy comparable to Carina or Ursa Minor would be marginally detectable in the 2MASS data. Extremely low-mass dSphs such as Ursa Major and And IX could therefore hide in the Galactic foreground below our detection limits, but there are no known dwarf irregular galaxies that contain as much gas as Complex H does and would not be detectable in 2MASS at a distance of 27 kpc. We conclude that Complex H would have to

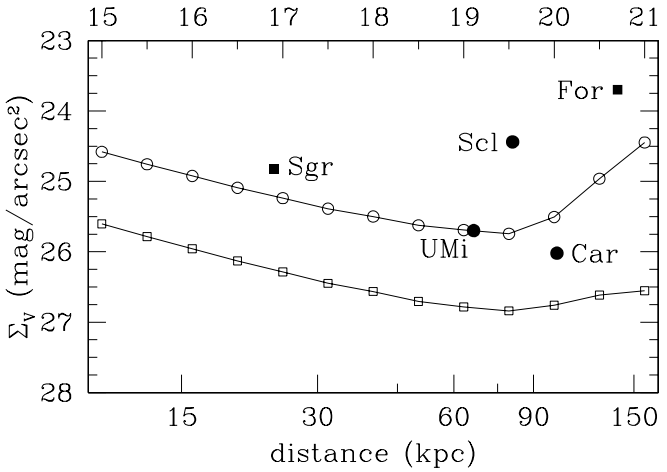

FIG. 7.— 3 σ detection limits for old and intermediate age stellar populations at the position of Complex H as a function of distance and surface brightness. The scale along the top of the figure shows distance modulus (in magnitudes). The open circles represent the detection limits for a dwarf containing only an old population of stars, and the open squares represent the detection limits if an intermediate-age population is present as well. For reference, the locations of a subset of known Milky Way satellites are shown with solid points — circles for the purely old systems (compare to the brighter detection limit), and squares for the mixed-age systems (compare to the fainter detection limit). Note that the surface brightnesses plotted for these galaxies represent the mean level over 1 deg^2, not the central surface brightness. At a distance of 27 kpc, the surface brightness limits are $\mu_V = 25.25$ mag arcsec^{-2} (old) and $\mu_V = 26.25$ mag arcsec^{-2} (intermediate), so the only known Local Group dwarfs that would not be detected at this position for reasonable distances are the very lowest-mass dwarf spheroidals (Carina, Sextans, Ursa Minor, Ursa Major, and And IX).

be a unique hybrid dwarf galaxy, with a large gas mass and low surface brightness, in order to contain a stellar population that is not visible in the 2MASS data.

A previous search of 2MASS data for an RGB associated with Complex H was carried out by S. Majewski and M. Skrutskie and also did not detect any evidence for a Complex H stellar population (Lockman 2003), consistent with our results.

4. DISCUSSION

4.1. *What Is Complex H?*

W98 presented six plausible explanations of the origin of Complex H, ranging from the neutral edge of a superbubble in the outer Galaxy to a massive, distant intergalactic cloud in the Local Group. Given the distance limits discussed in §1, the remaining possibilities are (1) Complex H was produced by a Galactic fountain, (2) Complex H is an infalling extragalactic cloud, and (3) Complex H is a nearby dwarf galaxy. A Galactic fountain origin for Complex H cannot be ruled out entirely without absorption-line measurements, but the low metallicities of other HVCs (e.g., Lu et al. 1994a,b; Wakker et al. 1999; Wakker 2001; Richter et al. 2001; Sembach et al. 2002; Tripp et al. 2003) and its large mass and distance suggest that this possibility is unlikely. To the remaining two possibilities, we add a third related, but distinct scenario: that Complex H represents gas that has been tidally stripped from a Milky Way satellite galaxy.

A stripped gas origin for Complex H also appears improbable for two reasons. First, the morphology of the HVC (Figure 1) does not appear consistent with that of a tidal stream. Rather than a highly elongated, symmetric structure (perhaps with sizeable remnant in the middle of it, if the progenitor has not been entirely destroyed), Complex H is asymmetric, with one end much denser than the other, and only moderately elongated (axis ratio of less than 2:1). The only way that Complex H could be a classical tidal stream is if the direction of the stream is along the line of sight. This orientation would seem to be at odds with the orbit discussed by Lockman (2003), which is roughly circular and inclined by 45° with respect to the Galactic plane, indicating that the direction of motion of Complex H is primarily perpendicular to the line of sight. The second difficulty with the tidal explanation is the lack of a credible progenitor object. Unlike the one HVC feature that is known to result from stripping of a dwarf galaxy, the Magellanic Stream, there are no known dwarf galaxies connected to any part of Complex H. Depending on the initial characteristics of this putative object (stellar mass, and relative extents of the gas and stars), one might expect a significant fraction of the stellar component to still be present at the location of the gas; the results of this paper rule such a possibility out. Therefore, the original stellar component must either be spread out in a stream along the orbit or exist as a bound object elsewhere on the orbit.

Complex H does not appear to host either significant amounts of recent star formation or a substantial old stellar population, making it difficult to distinguish between the two remaining possibilities. If Complex H is associated with a dwarf galaxy, it must be a rather faint dwarf to have escaped detection. The combination of a low total luminosity, small numbers of evolved stars, low levels of ongoing star formation, and a large gas mass would make this dwarf galaxy unique in the Local Group.

On the other hand, if Complex H is *not* a dwarf galaxy, we would be forced to conclude by default that it is an infalling extragalactic cloud that is in the process of being accreted by the Milky Way. In this case, we must understand why Complex H has failed to form any stars despite the $\gtrsim 10^7$ M$_\odot$ of H I that it contains. What makes Complex H different from other gas clouds of similar masses? Did it only acquire its gas recently, not allowing time for star formation? Is its internal pressure too low for molecular clouds to form (Blitz & Rosolowsky 2004)? Higher resolution H I observations of Complex H support the latter possibility, indicating peak H I column densities of $\sim 2.5 \times 10^{20}$ cm^{-2} and number densities of a few particles per cm^3 (Wakker & Schwarz 1991; Wakker, Vijfschaft, & Schwarz 1991; Lockman 2003). However, these measurements do not address the more fundamental issue of *why* the pressure and density in such a large cloud of gas are so low.

The key question that must be answered to resolve this issue is whether Complex H is surrounded by a dark matter halo, and therefore represents CDM sub-

structure, or whether it is a cold accretion flow such as those recently suggested by Birnboim & Dekel (2003), Keres et al. (2004), and Dekel & Birnboim (2004). The argument for Complex H being a dark galaxy relies on the CDM prediction of large numbers of low-mass dark matter halos, its large H I mass, and its almost unprecedented H I-to-stellar mass ratio. If the predicted subhalos exist (as we argue is likely; see §4.3), then the most massive subhalos should have retained or accreted some gas. Complex H seems to have many of the expected properties of one of these objects. The only hole in this case is the kinematics of the cloud. As described in §1, a cloud as massive as Complex H should have a rotation velocity of ~ 30 km s^{-1}, implying a velocity gradient as large as 60 km s^{-1}, or a velocity dispersion of similar magnitude. The observed gradient across the HVC is closer to 20 km s^{-1}, and the velocity dispersion is about 12 km s^{-1}, much smaller than expected. These values can still be compatible with a large total mass for Complex H if (1) we are seeing the rotation close to face-on, and therefore underestimating its amplitude, or (2) the H I is confined to the central regions of the dark matter halo, so that the kinematics do not reveal the full mass of the cloud. It is worth noting that other Local Group dwarfs with similar H I masses to Complex H (e.g., Sextans B and IC 1613) also have fairly low rotation amplitudes (~ 10 km s^{-1}) and velocity dispersions.

Because this interpretation requires somewhat special circumstances, the alternative possibility that Complex H represents an instance of "cold mode" gas accretion onto the Milky Way (as opposed to the standard "hot mode", in which gas is shock heated to very high temperatures and ionized at large radii before accreting onto a galaxy and later cooling) must be considered as well. Complex H would be the first observed example of this process, which has heretofore only been seen in hydrodynamic simulations. This would constitute strong evidence that cold accretion actually does play an important role in galaxy formation in the real universe. In addition to the kinematics, another piece of evidence in support of this idea is that Complex H is located relatively close on the sky to M31, which corresponds to the direction along the filament from which the Local Group formed (Blitz et al. 1999; Klypin et al. 2003). However, there are also problematic aspects to this picture, notably that Complex H cannot be gravitationally bound without large amounts of dark matter, and therefore would necessarily be a transient object that formed recently, and also that similar objects have not been detected around other galaxies even though surveys with sufficient sensitivity to detect Complex H analogs have been carried out. More detailed observations of the kinematics of Complex H may help to determine which of these possibilities is correct, but the more basic problem that the behavior of gas clouds in the Local Group is not yet understood (Sternberg et al. 2002) also must be addressed.

4.2. *Implications for the Nature of HVCs*

Complex H now joins an increasingly long list of other high-velocity clouds that appear not to contain stars (Simon & Blitz 2002; Davies et al. 2002; Willman et al. 2002b; Hopp et al. 2003; Siegel et al. 2005). The hypothesis that HVCs are the H I counterparts of normal low-surface brightness dwarf galaxies can therefore safely be put to rest. It remains possible, of course, that HVCs could host stellar populations whose surface brightness is significantly lower than that of any currently known galaxy, but more likely, HVCs simply do not contain any stars.

A number of competing models to explain the origins of HVCs have been proposed in recent years: (1) HVCs are distant ($d \gtrsim 500$ kpc), massive clouds that are the left-over building blocks of the Local Group (Blitz et al. 1999), (2) HVCs are small, nearby ($d \lesssim 50$ kpc) clouds that represent tidal debris from destroyed dwarf galaxies, and (3) HVCs are low-mass clouds at intermediate distances ($d \lesssim 150$ kpc) that are cooling and condensing out of the halo of hot gas that surrounds the Milky Way (Maller & Bullock 2005). Only in the first model would HVCs be expected to be associated with dwarf galaxies. The absence of stars in HVCs, however, is not necessarily evidence against this model because of the many possible mechanisms for suppressing star formation in low-mass objects (see §1). Our results therefore do not provide us with significant new leverage on the nature of HVCs. Still, it may be worth noting that Complex H is cooler ($T \sim 50$ K; Wakker et al. 1991) and possibly more massive than the clouds expected in the Maller & Bullock (2005) model.

4.3. *Implications for the Substructure Problem*

According to ΛCDM numerical simulations, the Local Group should contain up to ~ 500 low-mass dark matter halos (Klypin et al. 1999; Moore et al. 1999). Observationally, there are less than 40 known Local Group dwarf galaxies (e.g., Mateo 1998; van den Bergh 2000). Possible explanations for this mismatch are: (1) the simulations are overpredicting the amount of substructure that should be present, (2) there are many faint Local Group dwarfs that have not yet been discovered, or (3) ~ 90 % of low-mass halos never form stars. There are only a few ways to alter the predictions of the simulations, such as changing the initial power spectrum of density fluctuations (Kamionkowski & Liddle 2000) or imbuing the dark matter particles with new properties (e.g., a nonzero self-interaction cross-section [Spergel & Steinhardt 2000] or annihilation rate [e.g., Kaplinghat et al. 2000]). Because there is little theoretical or observational motivation for these ideas at present, much of the attention has focused on the other two potential solutions of the substructure problem.

Recent observational work has cast doubt on the idea that hundreds of undiscovered dwarf galaxies could exist in the Local Group. Willman et al. (2004) estimate that at most ~ 9 galaxies similar to the population of known Local Group dwarfs may still remain undiscovered around the Milky Way as a result of extinction and insufficient sensitivity at large radii. Our results reported here, along with the optical studies of other HVCs cited above (§4.2), show that HVCs do not contain dwarf galaxy-like stellar populations. The most straightforward interpretation of these findings is that there are no stars in HVCs; if any stars have formed, the process must have been extremely inefficient. We therefore argue that the substructure problem likely originates in the difficulty that low-mass dark matter halos experience in becoming dwarf galaxies. A number of theoretical ideas support the plausibility of this hypothesis. For example,

the heating of the intergalactic medium that occurred during the epoch of reionization may have prevented low-mass halos from holding on to their gas (Bullock et al. 2000). Simple photoionization caused by the ultraviolet background can also prevent these halos from forming stars (Somerville 2002). Tidal stripping may have removed most of the mass from dwarf galaxies relatively early in the history of the universe (Kravtsov et al. 2004). Alternatively, the supernova-driven winds produced by the formation of massive galaxies at high redshift could have blown out the interstellar medium of their satellite galaxies (Scannapieco et al. 2000, 2001).

Observations are also beginning to provide evidence in favor of this picture as well. Flux anomalies in multiply-imaged quasars appear to require that the lensing galaxies contain significant substructure (Mao & Schneider 1998; Chiba 2002; Metcalf & Zhao 2002; Dalal & Kochanek 2002; Kochanek & Dalal 2004). It is not yet clear whether these substructures are luminous or dark, but their abundance is roughly consistent with ΛCDM predictions. In the nearby universe, Robishaw, Simon, & Blitz (2002) recently identified a mysterious object that may be the first of the posited dark galaxies to be discovered in the Local Group. This object is a high-velocity cloud (HVC 127−41−330) that is apparently interacting with the Local Group dwarf galaxy LGS 3 and therefore is located at a distance of ~ 700 kpc from the Milky Way. The velocity field of this HVC indicates that it is rotating, and the inferred total mass is at least four times as large as the H I mass. A preliminary search for stars in HVC 127−41−330 did not yield any evidence for a stellar component (Robishaw et al. 2002), leading us to conclude that this object has all of the expected characteristics of one of the missing dark matter halos from CDM simulations (Simon, Robishaw, & Blitz 2003). Thilker et al. (2004) and Westmeier, Braun, & Thilker (2005) also argue that some, although not all, of the newly discovered HVCs around M31 may be dark matter-dominated Local Group subhalos.

Despite this apparently promising support for the possibility of inefficient star formation in low-mass objects resolving the substructure problem, it is worth noting that several extremely faint and low surface brightness objects have recently been discovered in the Sloan Digital Sky Survey, suggesting that the census of luminous dwarfs in the Local Group is not yet complete (Zucker et al. 2004; Willman et al. 2005a,b).

4.4. *Starless H I Clouds in the Local Group*

Do dark galaxies actually exist? Blind H I surveys covering large areas of sky and smaller targeted surveys of nearby galaxy groups have turned up small numbers of low-mass H I clouds, but deep optical imaging almost invariably reveals that these objects are associated with dwarf galaxies (e.g., Banks et al. 1999; Pisano, Wilcots, & Liu 2002). The only exception is the object recently announced by Minchin et al. (2005), VirgoHI21. This 10^8 $M_\odot$ cloud in the Virgo cluster has no optical counterpart down to a surface brightness limit of $\mu_B = 27.5$ mag arcsec^{-2}, which would make it the lowest surface brightness galaxy known if it does turn out to contain any stars. VirgoHI21 is currently the only such starless cloud known outside the Local Group, and therefore by default represents the closest extragalactic analog to Complex H, despite its large mass and location in a cluster environment. Minchin et al. (2005) suggest that previous H I surveys have not reached low enough column density limits to detect other similar objects, so more sensitive H I surveys may yet reveal a larger population of starless H I clouds (however, see Zwaan & Briggs 2000; Zwaan 2001).

Based on a thermal instability model of gas clouds embedded in dark matter halos, Taylor & Webster (2005) conclude that objects with H I masses comparable to Complex H are likely ($> 50\%$ probability) to form stars. However, the minimum self-regulating star formation rate that they predict for a 10^7 $M_\odot$ cloud is $\sim 10^{-6}$ $M_\odot$ yr^{-1}, significantly below the level that we would be able to detect; this model therefore does not require Complex H to be completely starless.

If Complex H and HVC 127−41−330 indeed lack any stellar component, then these clouds, along with Wright's Cloud (Wright 1974, 1979) and Davies' Cloud (Davies 1975), may be the most massive examples of a population of starless clouds of gas in the Local Group. It is tempting to associate these objects with some of the dark matter substructures predicted by CDM, but further kinematical studies will be necessary to determine whether Complex H, Wright's Cloud, and Davies' Cloud are in fact dark matter–dominated. The association of these objects with dark matter halos would provide strong evidence that the CDM substructure predictions are correct and that many more low-mass halos do exist in the Local Group, although the lower-mass halos may contain much less neutral gas (or none at all), making them more difficult to detect. Future multiwavelength investigations of these massive H I clouds to ascertain how they are distinct from similar-sized clouds that formed dwarf galaxies will help to illuminate the process of galaxy formation at both high and low redshift.

5. CONCLUSIONS

We have sought infrared and radio evidence of a dwarf galaxy associated with the massive, nearby HVC Complex H. Lockman (2003) showed that Complex H is most likely located slightly beyond the edge of the Milky Way disk at a distance of 27 ± 9 kpc from the Sun, consistent with the nondetection of high-velocity absorption lines in the spectra of distant OB stars (Wakker et al. 1998). Mid-infrared observations from the MSX satellite reveal many star-forming regions in the Galactic plane near the position of Complex H. We used CO observations to measure the velocities of 59 such sources and determined that they are clearly Milky Way objects. Only one of the sources was not detected in CO and therefore has an unknown origin, but it is plausible that our observations happened to miss the Milky Way CO cloud near this line of sight. Under the assumptions that Complex H lies at the distance of 27 kpc suggested by Lockman (2003), and that the Galactic CO-H_2 conversion factor applies to HVCs, we placed 3 σ upper limits of $24 - 130$ $M_\odot$ on the amount of molecular gas that could be present in Complex H at the position of each of these targets. These limits allow us to rule out the possibility that any of the infrared sources are associated with typical star-forming molecular cores or giant molecular clouds in Complex H. We also derived an up-

per limit of ~ 1000 $M_\odot$ on the mass of diffuse molecular gas that Complex H could contain. Assuming that there are no massive star-forming regions comparable to those in other Local Group dwarfs currently present in Complex H, as these observations suggest, we placed upper limits on the star formation rate in the HVC of 5×10^{-4} $M_\odot$ yr^{-1}. An alternative calculation based on the observed correlations between infrared emission, radio continuum emission, and star formation surface density in galaxies and star-forming regions produces the much stricter limit of 1×10^{-7} $(d/27 \text{ kpc})^2$ $M_\odot$ yr^{-1}. If the actual star formation rate in the HVC is close to the higher of these limits, Complex H would rank near the bottom of the list of Local Group dwarf irregulars in star formation despite its large reservoir of atomic gas.

We also used 2MASS data to constrain the possible intermediate and old stellar populations within Complex H. Near-infrared color-magnitude diagrams of the core of the HVC do not contain any detectable excess of RGB or AGB stars compared to a nearby control field. We built model stellar components for dwarf galaxies with purely old and old+intermediate populations and added them to the color-magnitude diagram of the control field to test their detectability. We determined that the nondetection of Complex H in 2MASS places a lower limit of $\mu_V = 25.25$ mag arcsec^{-2} on its intrinsic surface brightness (assuming a distance of 27 kpc), indicating that most of the known dwarf galaxies in the Local Group (and all of the known dwarfs with gas) could be detected at the position of Complex H. The corresponding upper limit to the stellar mass of Complex H is 10^6 $M_\odot$, assuming a V-band stellar mass-to-light ratio of 2. If a significant intermediate-age population is present as well, the surface brightness limit improves to 26.25 mag arcsec^{-2}, and the stellar mass limit is even lower.

While we cannot entirely rule out the existence of a dwarf galaxy associated with Complex H, these results demonstrate that the galaxy must have a unique set of properties and a rather low surface brightness if it exists. There are no known dwarfs that have the combined characteristics of a large gas mass, very low current rates of star formation, and a very small intermediate and old stellar population. If Complex H does contain any stars, it almost certainly has the largest $M_{\rm H\,I}/L_B$ and one of the smallest populations of evolved stars in the Local Group.

We presented arguments that Complex H is either a dark galaxy in the Local Group, or an example of a cold accretion flow onto the Milky Way. In either case, this HVC is a unique object whose existence has important implications for our understanding of galaxy formation, and further observations and modeling will be needed to determine the true nature of Complex H. If Complex H is a dark galaxy, and the Cold Dark Matter prediction of hundreds of low-mass dark matter halos in the Local Group is correct, then our results provide observational evidence that these halos may be unable to form stars. Some of the most massive subhalos, such as Complex H and the dark matter–dominated HVC described by Robishaw et al. (2002) may have accumulated enough gas to be detected as high-velocity clouds, but the bulk of the population could remain entirely dark.

This research was partially supported by NSF grants AST-9981308 and AST-0228963. The authors acknowledge the referee, Steven Majewski, for suggestions that helped to clarify and improve the paper. JDS would like to thank Tam Helfer for her introduction to COMB and observing with the 12 m. We also acknowledge the assistance of telescope operators Duane Clark and Kevin Long and express appreciation for their ability to keep the telescope running. JDS also thanks Tim Robishaw for his usual assistance with IDL-related matters. MC thanks NASA for supporting his participation in this work under LTSA grant NAG5-7936 with UC Berkeley. This work makes use of data products from the Midcourse Space Experiment. Processing of the data was funded by the Ballistic Missile Defense Organization with additional support from the NASA Office of Space Science. This publication also makes use of data products from the Two Micron All Sky Survey, which is a joint project of the University of Massachusetts and the Infrared Processing and Analysis Center/California Institute of Technology, funded by the National Aeronautics and Space Administration (NASA) and the National Science Foundation. This research has also made use of NASA's Astrophysics Data System Bibliographic Services.

REFERENCES

Banks, G. D., et al. 1999, ApJ, 524, 612
Birnboim, Y., & Dekel, A. 2003, MNRAS, 345, 349
Blitz, L., & Robishaw, T. 2000, ApJ, 541, 675
Blitz, L., & Rosolowsky, E. 2004, ApJ, 612, L29
Blitz, L., Spergel, D. N., Teuben, P. J., Hartmann, D., & Burton, W. B. 1999, ApJ, 514, 818
Bolatto, A. D., Leroy, A., Israel, F. P., & Jackson, J. M. 2003, ApJ, 595, 167
Bullock, J. S., Kravtsov, A. V., & Weinberg, D. H. 2000, ApJ, 539, 517
Carpenter, J. M., Heyer, M. H., & Snell, R. L. 2000, ApJS, 130, 381
Chandar, R., Bianchi, L., & Ford, H. C. 2000, AJ, 120, 3088
Chiba, M. 2002, ApJ, 565, 17
Cole, A. A. 2001, ApJ, 559, L17
Cohen, M., & Green, A. J. 2001, MNRAS, 325, 531
Cohen, M., Staveley-Smith, L., & Green, A. 2003, MNRAS, 340, 275
Cutri, R. M., et al. 2003, VizieR Online Data Catalog, 2246, 0
Dalal, N., & Kochanek, C. S. 2002, ApJ, 572, 25
Davidge, T. J. 2000, PASP, 112, 1177
—. 2000, AJ, 120, 1853
Davies, J., Sabatini, S., Davies, L., Linder, S., Roberts, S., Smith, R., & Evans, R. 2002, MNRAS, 336, 155
Davies, R. D. 1975, MNRAS, 170, 45P
Dekel, A., & Birnboim, Y. 2004 (preprint: astro-ph/0412300)
Dekel, A., & Woo, J. 2003, MNRAS, 344, 1131
Dieter, N. H. 1971, A&A, 12, 59
Digel, S., de Geus, E., & Thaddeus, P. 1994, ApJ, 422, 92
Efstathiou, G. 1992, MNRAS, 256, 43P
Egan, M. P., et al. 2003, AFRL Tech. Rep. No. AFRL-VS-TR-2003-1589
Fich, M., & Terebey, S. 1996, ApJ, 472, 624
Filipovic, M. D., Haynes, R. F., White, G. L., & Jones, P. A. 1998, A&AS, 130, 421
Girardi, L., Bressan, A., Bertelli, G., & Chiosi, C. 2000, A&AS, 141, 371
Gómez, G. C., Benjamin, R. A., & Cox, D. P. 2002, Revista Mexicana de Astronomia y Astrofisica Conference Series, 12, 39
Hartmann, D., & Burton, W. B. 1997, Atlas of Galactic Neutral Hydrogen (Cambridge; New York: Cambridge University Press, ISBN 0521471117)
Heydari-Malayeri, M., Rosa, M. R., Zinnecker, H., Deharveng, L., & Charmandaris, V. 1999, A&A, 344, 848
Hodge, P., & Lee, M. G. 1990, PASP, 102, 26
Hopp, U., Schulte-Ladbeck, R. E., & Kerp, J. 2003, MNRAS, 339, 33
Hulsbosch, A. N. M. 1971, A&A, 14, 489

Ibata, R. A., Gilmore, G., & Irwin, M. J. 1995, MNRAS, 277, 781
Irwin, M., & Hatzidimitriou, D. 1995, MNRAS, 277, 1354
Ivezic, Z., & Christodoulou, D. M. 1997, ApJ, 486, 818
Joncas, G., Durand, D., & Roger, R. S. 1992, ApJ, 387, 591
Kamionkowski, M., & Liddle, A. R. 2000, Physical Review Letters, 84, 4525
Kaplinghat, M., Knox, L., & Turner, M. S. 2000, Physical Review Letters, 85, 3335
Kennicutt, R. C., Tamblyn, P., & Congdon, C. E. 1994, ApJ, 435, 22
Keres, D., Katz, N., Weinberg, D. H., & Dave, R. 2004, submitted to MNRAS (preprint: astro-ph/0407095)
Klypin, A., Hoffman, Y., Kravtsov, A. V., & Gottlöber, S. 2003, ApJ, 596, 19
Klypin, A., Kravtsov, A. V., Valenzuela, O., & Prada, F. 1999, ApJ, 522, 82
Kochanek, C. S., & Dalal, N. 2004, ApJ, 610, 69
Kravtsov, A. V., Gnedin, O. Y., & Klypin, A. A. 2004, ApJ, 609, 482
Kroupa, P. 2001, MNRAS, 322, 231
Lequeux, J., Peimbert, M., Rayo, J. F., Serrano, A., & Torres-Peimbert, S. 1979, A&A, 80, 155
Lockman, F. J. 2003, ApJ, 591, L33
Lu, L., Savage, B. D., & Sembach, K. R. 1994a, ApJ, 426, 563
—. 1994b, ApJ, 437, L119
Maller, A. H., & Bullock, J. S. 2005, MNRAS, in press
Mao, S,. & Schneider, P. 1998, MNRAS, 295, 587
Mateo, M. L. 1998, ARA&A, 36, 435
Metcalf, R. B., & Zhao, H. 2002, ApJ, 567, L5
Mill, J. D., et al. 1994, Journal of Spacecraft and Rockets, 31, 900
Minchin, R., et al. 2005, ApJ, in press (preprint: astro-ph/0502312)
Moore, B., Ghigna, S., Governato, F., Lake, G., Quinn, T., Stadel, J., & Tozzi, P. 1999, ApJ, 524, L19
Murgia, M., Crapsi, A., Moscadelli, L., & Gregorini, L. 2002, A&A, 385, 412
Nikolaev, S., & Weinberg, M. D. 2000, ApJ, 542, 804
Peimbert, M., & Torres-Peimbert, S. 1976, ApJ, 203, 581
Pisano, D. J., Wilcots, E. M., & Liu, C. T. 2002, ApJS, 142, 161
Price, S. D., Egan, M. P., Carey, S. J., Mizuno, D. R., & Kuchar, T. A. 2001, AJ, 121, 2819
Richter, P., Sembach, K. R., Wakker, B. P., Savage, B. D., Tripp, T. M., Murphy, E. M., Kalberla, P. M. W., & Jenkins, E. B. 2001, ApJ, 559, 318
Robishaw, T., Simon, J. D., & Blitz, L. 2002, ApJ, 580, L129
Rosolowsky, E., Engargiola, G., Plambeck, R., & Blitz, L. 2003, ApJ, 599, 258
Salpeter, E. E. 1955, ApJ, 121, 161
Saviane, I., Held, E. V., & Bertelli, G. 2000, A&A, 355, 56
Scannapieco, E., Ferrara, A., & Broadhurst, T. 2000, ApJ, 536, L11
Scannapieco, E., Thacker, R. J., & Davis, M. 2001, ApJ, 557, 605
Schlegel, D. J., Finkbeiner, D. P., & Davis, M. 1998, ApJ, 500, 525
Sembach, K. R., Gibson, B. K., Fenner, Y., & Putman, M. E. 2002, ApJ, 572, 178
Sharpless, S. 1959, ApJS, 4, 257
Siegel, M. H., et al. 2005, ApJ, in press (preprint: astro-ph/0412699)
Simon, J. D., & Blitz, L. 2002, ApJ, 574, 726
Simon, J. D., Robishaw, T., & Blitz, L. 2003, in ASP Conference Series: Satellites and Tidal Streams
Somerville, R. S. 2002, ApJ, 572, L23
Spergel, D. N., & Steinhardt, P. J. 2000, Physical Review Letters, 84, 3760
Sternberg, A., McKee, C. F., & Wolfire, M. G. 2002, ApJS, 143, 419
Taylor, E. N., & Webster, R. L. 2005, submitted to ApJ (preprint: astro-ph/0412699)
Thilker, D. A., Braun, R., Walterbos, R. A. M., Corbelli, E., Lockman, F. J., Murphy, E., & Maddalena, R. 2004, ApJ, 601, L39
Tripp, T. M., et al. 2003, AJ, 125, 3122
van den Bergh, S. 2000, PASP, 112, 529
Verde, L., Oh, S. P., & Jimenez, R. 2002, MNRAS, 336, 541
Wakker, B., van Woerden, H., de Boer, K. S., & Kalberla, P. 1998, ApJ, 493, 762
Wakker, B. P. 2001, ApJS, 136, 463
Wakker, B. P., & Schwarz, U. J. 1991, A&A, 250, 484
Wakker, B. P., & van Woerden, H. 1991, A&A, 250, 509
Wakker, B. P., Vijfschaft, B., & Schwarz, U. J. 1991, A&A, 249, 233
Wakker, B. P., et al. 1999, Nature, 402, 388
Walter, F., Taylor, C. L., Hüttemeister, S., Scoville, N., & McIntyre, V. 2001, AJ, 121, 727
Walter, F., Weiss, A., Martin, C., & Scoville, N. 2002, AJ, 123, 225
Westmeier, T., Braun, R., & Thilker, D. 2005, A&A, 436, 101
Willman, B., Dalcanton, J., Ivezić, Ž., Jackson, T., Lupton, R., Brinkmann, J., Hennessy, G., & Hindsley, R. 2002, AJ, 123, 848
Willman, B., Dalcanton, J., Ivezić, Ž., Schneider, D. P., & York, D. G. 2002, AJ, 124, 2600
Willman, B., Governato, F., Dalcanton, J. J., Reed, D., & Quinn, T. 2004, MNRAS, 353, 639
Willman, B., et al. 2005a, AJ, in press (preprint: astro-ph/0410416)
Willman, R., et al. 2005b, submitted to ApJ (preprint: astro-ph/0503552)
Wright, M. C. H. 1974, A&A, 31, 317
—. 1979, ApJ, 233, 35
Zucker, D. B., et al. 2004, ApJ, 612, L121
Zwaan, M. A. 2001, MNRAS, 325, 1142
Zwaan, M. A., & Briggs, F. H. 2000, ApJ, 530, L61

TABLE 1
Milky Way CO Lines Detected Toward Mid-Infrared Sources

ℓ (1)	b (2)	V_{LSR} (km s^{-1}) (3)	T_b (K) (4)	I_{CO} (K km s^{-1}) (5)	Source (6)
126.03	−0.32	−47.0	5.84	8.16	MSXE
126.34	0.48	1.9	4.89	5.35	MSXE
		−4.6	1.49	1.89	
		−12.8	3.61	10.66	
		−45.3	1.65	2.23	
126.41	4.61	3.8	2.15	2.78	MSXE
		−6.5	0.97	2.01	
		−9.8	0.51	0.50	
126.42	1.79	−11.5	0.52	0.41	MSXE
		−46.2	0.41	0.59	
126.43	1.02	1.4	−0.65	−1.30	MSXE
		−67.2	0.95	1.10	
126.58	0.20	−11.9	2.99	5.15	MSXE
		−13.1	−2.85	−6.56	
		−52.9	1.10	1.15	
126.83	0.94	−10.5	2.42	3.95	MSXE
		−36.3	1.65	1.99	
		−54.0	−0.83	−1.03	
126.98	1.07	−37.0	2.11	3.28	MSXE
		−53.9	1.02	1.59	
127.03	0.76	−41.9	12.02	19.70	MSXE
		−51.0	0.40	0.77	
127.16	−0.53	−13.3	−2.46	−2.12	MSXE
		−44.5	5.96	12.74	
		−53.8	1.28	1.45	

TABLE 1 — *Continued*

ℓ (1)	b (2)	V_{LSR} (km s^{-1}) (3)	T_b (K) (4)	I_{CO} (K km s^{-1}) (5)	Source (6)
		−56.1	−3.35	−3.49	
127.16	1.87	−1.1	2.11	5.45	MSXE
127.21	0.98	−43.0	9.04	22.61	MSXE
		−52.1	2.98	3.37	
127.45	0.67	9.4	1.80	5.93	MSXE
		−52.5	1.74	2.69	
127.45	0.52	−34.4	3.73	4.60	MSXE
		−50.4	1.47	3.13	
127.48	0.98	−39.7	8.56	8.99	MSXE
127.49	1.16	−36.0	0.51	0.57	MSXE
		−52.1	0.61	1.31	
		−58.2	0.37	0.80	
127.62	0.89	−41.5	7.08	8.04	MSXE
		−51.7	1.28	1.61	
127.78	0.61	8.1	1.22	2.41	MSXE
127.84	1.70	−55.4	2.08	2.40	MSXE
127.86	1.16	−59.8	2.57	6.34	MSXE
		−53.8	1.68	2.95	
127.98	4.69	−8.7	2.93	4.41	MSXE
128.17	−0.45	−12.7	2.51	4.67	MSXE
		−41.7	3.67	5.48	
128.18	3.59	−8.9	2.31	2.11	MSXE
128.55	1.24	−51.1	1.71	3.36	MSXE
		−52.9	1.06	0.87	
128.82	1.59	−7.8	1.57	1.67	MSXE
		−10.0	1.27	1.58	
		−55.7	2.65	4.02	
		−82.2	1.71	2.60	
129.81	1.43	−38.4	1.86	4.15	MSXE
		−55.0	1.21	1.51	
		−77.0	0.61	0.69	
		−82.2	0.82	0.88	
130.00	1.83	−47.2	3.71	3.76	MSXE
		−81.0	1.00	1.46	
130.13	1.91	2.4	1.10	1.86	MSXE
130.18	0.53	−10.9	2.38	2.76	MSXE
		−12.6	1.21	1.18	
		−45.6	0.86	1.10	
130.52	1.21	−66.0	0.57	0.83	MSXE
130.61	2.85	−7.4	−1.73	−2.33	MSXE
130.82	−0.02	−17.1	4.32	5.54	MSXE
		−33.0	3.38	4.07	
130.95	4.43	−14.1	1.78	2.87	MSXE
130.99	0.56	−30.8	1.91	3.18	MSXE
131.53	4.58	−33.1	6.67	11.48	MSXE
131.79	3.75	−8.2	−1.49	−1.50	MSXE
		−8.0	0.80	0.38	
		−40.7	−0.66	−1.21	
131.81	1.36	−57.4	1.22	1.69	MSXE
		−79.0	3.11	4.68	
131.94	1.82	−45.6	1.22	2.02	MSXE
		−69.9	0.89	1.60	
132.12	1.65	−75.0	0.43	0.88	MSXE
		−101.7	0.37	0.39	
132.16	3.84	−41.2	2.30	4.03	MSXE
132.17	2.29	−7.7	2.69	3.50	MSXE
		−73.7	0.67	0.75	
132.36	3.98	−41.1	1.80	2.65	MSXE
132.83	3.89	−1.5	1.24	1.48	MSXE
		−7.9	−1.06	−1.24	
		−9.6	3.05	2.71	
131.666	1.934	−41.2	0.44	0.44	MSXP
		−79.1	0.46	0.72	
131.856	1.331	−56.1	0.49	0.72	MSXP
		−78.7	8.38	23.94	
131.826	1.364	−56.3	0.38	0.43	MSXP
		−78.5	3.14	4.48	
130.294	1.654	−3.3	0.51	0.66	MSXP
		−54.5	6.04	9.95	
131.709	0.624	−2.7	2.21	6.50	MSXP
131.186	0.474	...	...	...	MSXP
131.136	0.164	−5.0	2.00	4.10	MSXP
		−19.0	0.30	0.86	
130.416	0.266	−9.1	0.69	0.44	MSXP
		−11.5	−4.65	−11.81	

TABLE 1 — *Continued*

ℓ (1)	b (2)	V_{LSR} (km s^{-1}) (3)	T_b (K) (4)	I_{CO} (K km s^{-1}) (5)	Source (6)
130.896	0.419	−58.9	2.20	5.48	MSXP
130.484	0.156	−11.5	−1.20	−1.91	MSXP
		−88.7	0.40	0.87	
130.294	1.654	−54.5	6.49	10.34	MSXP
126.43	4.48	2.2	3.82	6.25	FT96
		−10.2	2.23	5.69	
127.09	1.86	−0.4	2.66	3.63	FT96
		−2.9	1.38	1.53	
		−8.1	1.00	0.64	
127.83	1.67	−7.3	1.17	1.81	FT96
		−57.7	4.38	4.23	
		−87.3	−1.30	−1.98	
127.91	0.66	−63.4	6.55	19.10	FT96
128.78	2.01	−82.0	10.47	30.76	FT96
130.00	1.81	−43.5	0.59	0.86	FT96
		−47.2	2.89	2.96	
		−81.5	0.52	1.22	
130.29	1.66	−10.8	0.55	0.79	FT96
		−43.0	0.77	1.26	
		−54.5	3.45	6.05	